INHALATION TOXICOLOGY
https://doi.org/10.1080/08958378.2023.2267618

Taylor & Francis
Taylor & Francis Group

RESEARCH ARTICLE

OPEN ACCESS Check for updates

# Development of a non-target strategy for evaluation of potential biological effects of inhalable aerosols generated during purposeful room conditioning using an *in vitro* inhalation model

Detlef Ritter[a], Jan Knebel[a], Tanja Hansen[a], Anne Zifle[b], Anne Fuchs[b], Rolf Fautz[b] and Katharina Schwarz[a]

[a]Respiratory Pharmacology, Fraunhofer ITEM, Hannover, Germany; [b]KAO Germany, Darmstadt, Germany

**ABSTRACT**

Objectives: An integrated *in vitro* inhalation approach was outlined to estimate potential adverse acute inhalation effects of aerosols from commercial nebulizer applications used for purposeful room conditioning such as disinfection, scenting or others. Aerosol characterization, exposure estimation and evaluation of acute biological effects by *in vitro* inhalation were included to generate dose-response data, allowing for determination of *in vitro* lowest observable adverse effect levels (LOAELs). Correlation of these to estimates of human lung deposition was included for quantitative *in vitro* to *in vivo* extrapolation approach (QIVIVE) for acute effects during human exposure.

Methods: To test the proposed approach, a case study was undertaken using two realistic test materials. An acute *in vitro* inhalation setup with air-liquid interface A549-cells in an optimized exposure situation (P.R.I.T.® ExpoCube®) was used to expose cells and analysis of relevant biological effects (viability, mitochondrial membrane potential, stress, IL-8 release) was carried out. Results: The observed dose-responsive effects in a sub-toxic dose-range could be attributed to the main component of one test material and its presence in the aerosol phase of the nebulized material. QIVIVE resulted in a factor of at least 256 between the *in vitro* LOAEL and the estimated acute human lung exposure for this test material.

Conclusions: The case-study shows the value of the non-target *in vitro* inhalation testing approach especially in case of a lack of knowledge on complex product composition. It is expected that approaches like this will be of high value for product safety and environmental health in the future.

**ARTICLE HISTORY**
Received 7 November 2022
Accepted 29 September 2023

**KEYWORDS**
Inhalation; in vitro; acute toxicity; non-target; aerosol

**HIGHLIGHTS**

- Design of a routine *in vitro* inhalation approach to estimate biological effects of nebulized products.
- Application in a case study on a potential real product for purposeful room conditioning by use of a commercial nebulizer.
- Combining results from aerosol characterization and *in vitro* inhalation experiments allowed for comprehensive correlation of product composition, aerosol properties and biological effects.
- Assignment of sub-toxic biological effects to a specific product component enabled identification of a product composition with potentially even less biological effect.
- Combined *in vivo* exposure estimation and *in vitro* LOAEL determination enabled a QIVIVE approach.

**Abbreviations:** ADME: absorption, distribution, metabolism and excretion; AE-Box: aerosol extraction box; A549: human alveolar lung cell line; ATCC: American type culture collection; LOAEL: lowest observable adverse effect level; FBS: fetal bovine serum; QIVIVE: quantitative *in vitro* to *in vivo* extrapolation; ALI: air-liquid interface; COVID-19: corona virus disease 2019; GRAS: generally recognized as save; FDA: food and drug agency; e-cigarette: electronic cigarette; ED50: 50% effective dose; FT-IR: fourier-transform infrared spectroscopy; WST-1: water-soluble tetrazolium; JC-1: mitochondrial membrane stain; IL-8: interleukin 8; ELISA: enzyme-linked immunosorbent assay; MMAD: mass median aerodynamic diameter; MTT: 3-(4,5-dimethylthiazole-2-yl)-2,5-diphenyltetrazoliumbromide; FACS: fluorescence-activated cell sorting; DNA: deoxyribonucleic acid; MPPD: mutiple-path particle dosimetry model; HCS: high-content screening; NOEL: no-observed-effect level; QIVIVE: quantitative *in vitro* to *in vivo* extrapolation

**CONTACT** Detlef Ritter detlef.ritter@item.fraunhofer.de Respiratory Pharmacology, Fraunhofer ITEM, Nikolai-Fuchs-Str. 1, D-30625 Hannover, Germany

## Introduction

Aerosols are released from several sources in the natural environment (e.g. fog, mists) from engine emissions (industrial sources, automobiles, heating, etc.) or at work places (welding fumes, etc.) but are also used for medical application as inhalable sprays to achieve effective and gentle treatment of lung-related diseases. Nowadays, aerosols are also applied for purposeful conditioning of indoor air, for example to disinfect or humidify room air or to release defined scents or smells. This might take place in shops or malls to set the customer into a favorable mood as a recent marketing strategy. Room disinfection by aerosols with chemically active ingredients has come up during the COVID-19 pandemic (Lou et al. 2021; Srivastava et al. 2021; Vlaskin 2022). Such aerosols can be technically set up using commercial nebulizers with a liquid filling. In the best case, all components of these liquids are known and toxicologically characterized. However, even in this case, the toxicological properties of the single components are usually only characterized for other routes than inhalation. This, for instance, is true for so-called GRAS substances, which are 'generally recognized as safe' for food application but are not necessarily tested for inhalation toxicity (Hallagan et al. 2020; FDA 2022). Moreover, liquids for nebulization usually represent very complex mixtures with different components for specific functionalities such as disinfection, humidification, generating scents ('active ingredient mixture') or dissolution or technical aerosol formation ('main components'). Even if the complete toxicological profile of all the single components would be known, it would not be possible to predict the final toxicological profile due to a lack of knowledge on the resulting toxicology of the complex mixture.

A case study is presented here as an approach for the development of a non-animal method to generate toxicological relevant data for safety assessment. Two test materials were studied as nebulizer fillings. They are used in a commercial nebulizer and represent potential products to be tested with only very limited knowledge on composition. Basically, they are composed of two main groups of compounds. A main ingredient acting as solvent or providing necessary technical properties to enable nebulization and an active ingredient mixture (scents, disinfectants, etc.) of unknown composition. Of these, test material 1 (TM1) contained 80% of a main component type 1 (MC1) and 20% of an active ingredient mix. Test material 2 (TM2) contained the same active ingredient mix (30%) but a different main component type 2 (MC2, 70%). Starting from this situation of very limited information, the strategy of the study was to generate as much experimental information as possible for potential further safety assessment. The method is aimed at future routine use for comparative testing of products or product variations.

We focused on local lung irritation as a potential risk, which might be induced by various ingredients of the nebulized fillings. The modes of action (MoA) for tissue irritation are in many cases nonspecific and diverse, a single adverse outcome pathway (AOP) can thus not be proposed. Consequently, lung irritation is understood in a 'non-target way' as any kind of significant biological change upon inhalation using well-known toxicological *in vitro* endpoints (e.g. viability and mitochondrial effects). Worst-case conditions were chosen to account for uncertainties in the approach for quantitative extrapolation from *in vitro* results to the *in vivo* exposure situation (QIVIVE, Hartung 2018). To achieve further relevance of the model by evaluation of effects below acute cell-toxic doses, analysis of an *in vitro* cellular stress parameter and interleukin-8 release was applied. Although sub-toxic events represent biological changes which do not have to be adverse by definition, they are likely to elicit relevance for long-term exposure *in vivo* and might contribute to toxicity, adverse physiological tissue effects or changes in the immune system in the long run. It is supposed that they might give information on potential biological effects beyond the 'acute exposure' setting which is usually defined by the limited exposure time possible in a 'routine' *in vitro* inhalation test model. There are still no well-established *in vitro* methods which might predict resulting long-term or so-called 'chronic' effects upon inhalation. Relatively laborious *in vitro* approaches such as long-term or repeated exposures (Person et al. 2013; Mennecier et al. 2014; Gindele et al. 2020; Bukowy-Bieryłło 2021) are applied to account for approximation of this aim, but are not suitable for a 'routine' test design.

Although only consisting of a single cell type from the human alveolar space, the human alveolar type-II-like A549 lung cell line (Lieber et al. 1976; Nardone and Andrews 1979) was chosen as a species- and organ-relevant cell model. It is well-characterized, extremely reproducible to handle, has shown promising qualities regarding the *in vitro* to *in vivo* prediction perspective, and thus, seems well-suited for the intended *in vitro* inhalation approach (Upadhyay and Palmberg 2018; Selo et al. 2021). Moreover, predictivity of viability read-outs for acute *in vivo* respiratory toxicity may be promising especially using the A549 cell line (Lim et al. 2021).

As a first step in the direction of *in vivo* prediction from *in vitro* results, a concept according to Figure 1 was outlined. It started with (I) the rough estimation of possible

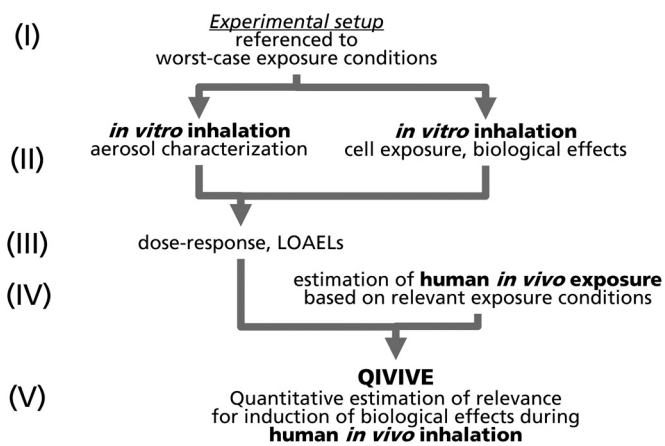


**Figure 1.** Concept for experimental design, starting from non-target *in vitro* inhalation exposure based on worst-case conditions and aiming at quantitative *in vitro* to *in vivo* extrapolation (QIVIVE).

real room concentrations using the relevant nebulizer, (II) use of these room concentrations for setting up relevant worst-case exposure scenarios for the *in vitro* inhalation model, (III) experimental identification of characteristic toxicological values ($ED_{50}$ values, LOAELs) from *in vitro* dose-response and finally comparison of the characteristic values to (IV) estimated real human exposure. The human exposure estimation was carried out based on more realistic calculation of equilibrium aerosol room concentrations during real use. Comparison of *in vitro* results and estimated human exposure enabled (V) discussion of a quantitative *in vitro* to *in vivo* extrapolation approach (QIVIVE).

In summary, the concept described here aimed on deriving as much toxicological information for potential risk assessment as possible using an alternative *in vitro* inhalation approach. The 'non-target' character is understood in two ways: (I) detection of biological effects which are not representative for specific toxicological mechanisms or correlated to AOPs and (II) biological effects occur as an effect of the exposure situation to nebulized relevant test mixtures without detailed knowledge on material composition. Due to the given situation of very limited information on ingredients, potential validation of the developed inhalation model could not be achieved by comparison of results to well-known toxicological data base profiles or literature data. Value of the approach for use of results in risk assessment is based on two aspects. First, evidence exists on the relevance of such *in vitro* models for *in vivo* prediction (Dwivedi et al. 2018; Lim et al. 2021; Di Ianni et al. 2021) and from using model substances in a comparable experimental setting (Ritter et al. 2018). Second, it was possible to include an experimental matrix consisting of different test situations to evaluate the conclusiveness of the results. This test matrix included dose-response testing using nebulized TM1 and experimental variations of the nebulized test materials such as filtering, using the pure main component from of nebulized TM1, only and nebulized TM2. By merging aerosol characteristics and dose-response data a high level of conclusiveness of the results could be shown.

## Materials and methods

### Aerosol generation

The reference target concentration for aerosol generation during the *in vitro* inhalation testing was based on a 'worst-case' assumption that neglected any physico-chemical processes resulting in a steady-state balance between generation and depletion (aggregation, settlement by gravitation, air change in the room and others). It was assumed that the complete aerosol produced by the nebulizer (Prolitec, Milwaukee, USA, Model AQ160) would stay airborne. Four concentration levels were set based on this assumption (CL1 – CL4). The basic 'worst-case' scenario for TM1 was defined based on the nebulizer output rate, a reference room size according to the manufacturers' advice and a continuous 1-day use (output rate 15 mg/min, room volume 135 $m^3$, 24 h) resulting in a value of 160 $mg/m^3$ total mass concentration. Concentration levels 1–4 were set using factors of 0.4×, 2×, or 6× of this basic concentration resulting in a range from 60 to 900 $mg/m^3$ as target total mass concentrations. Additional testing scenarios included filtering of the TM1 aerosol, the main component of TM1 only and TM2 (Table 1).

For aerosol generation during *in vitro* inhalation experiments, the primary aerosol flow from the nebulizer was conducted into a sheath flow of clean air and divided into a reduced flow, which was conducted into an aerosol box ('AE-box,' Ritter et al. 2018) followed by a final dilution with clean air (Figure 2). Flows (pre-dilution flow, reduction flow, final dilution flow) were in the ranges given in Figure 2(a) depending on the exposure scenario to meet the target total mass concentrations.

### Aerosol characterization

The primary droplet size of the aerosol from the nebulizer was measured by laser diffraction analysis (Malvern Spraytec, Malvern Panalyticel Ltd, GB, 300 mm lens, 0.1–900 µm (Dv50: 0.5–600 µm)). The 'total mass concentration' (total airborne material in gas and aerosol phase) was calculated from the mass of nebulized liquid and applied flow rates (primary flow, pre-dilution, delivered flow and final dilution, Figure 2(a)). The mass of nebulized liquid during cell exposure experiments was determined gravimetrically from the nebulizer cartridge. The 'actual aerosol concentration' in the AE-box was analyzed using gravimetrical filter analysis after sampling directly from the box. The 'relative aerosol concentration' [V] was followed using a custom light scattering photometer which was positioned directly in front of the cell exposure device. For 'filtered' scenarios, a filter (Munktell LP-050, Ahlstrom, Sweden, particle retention efficiency $\geq$99.998% (0.3 µm)) was positioned in front of photometer and cell exposure device. Hence, the photometer validated the filter performance, while gravimetrical filter analysis of the original source aerosol was still possible directly from the box. For analysis of the gas phase concentration of the exposure atmosphere only ('relative gas

**Table 1.** Exposure scenarios using nebulized TM1 and TM2, filtered aerosol and the pure main component from TM1.

| Test material | Concentration level | Target total mass concentration [$mg/m^3$] | Basic scenarios | Test material | Concentration level | Target total mass concentration [$mg/m^3$] | Additional scenarios |
|---|---|---|---|---|---|---|---|
| 1 | 1 | 60 | TM1-CL1 | 1 (filtered) | 2 | 160 | TM1 (filt.)-CL2 |
| 1 | 2 | 160 | TM1-CL2 | 1 (filtered) | 4 | 900 | TM1 (filt.)-CL4 |
| 1 | 3 | 300 | TM1-CL3 | 1 (main component only) | 2 | 160 | TM1 (mc)-CL2 |
| 1 | 4 | 900 | TM1-CL4 | 1 (main component only) | 4 | 900 | TM1 (mc)-CL4 |
| | | | | 2 | 2 | 160 | TM2 (filt.)-CL2 |
| | | | | 2 | 4 | 900 | TM2 (filt.)-CL4 |

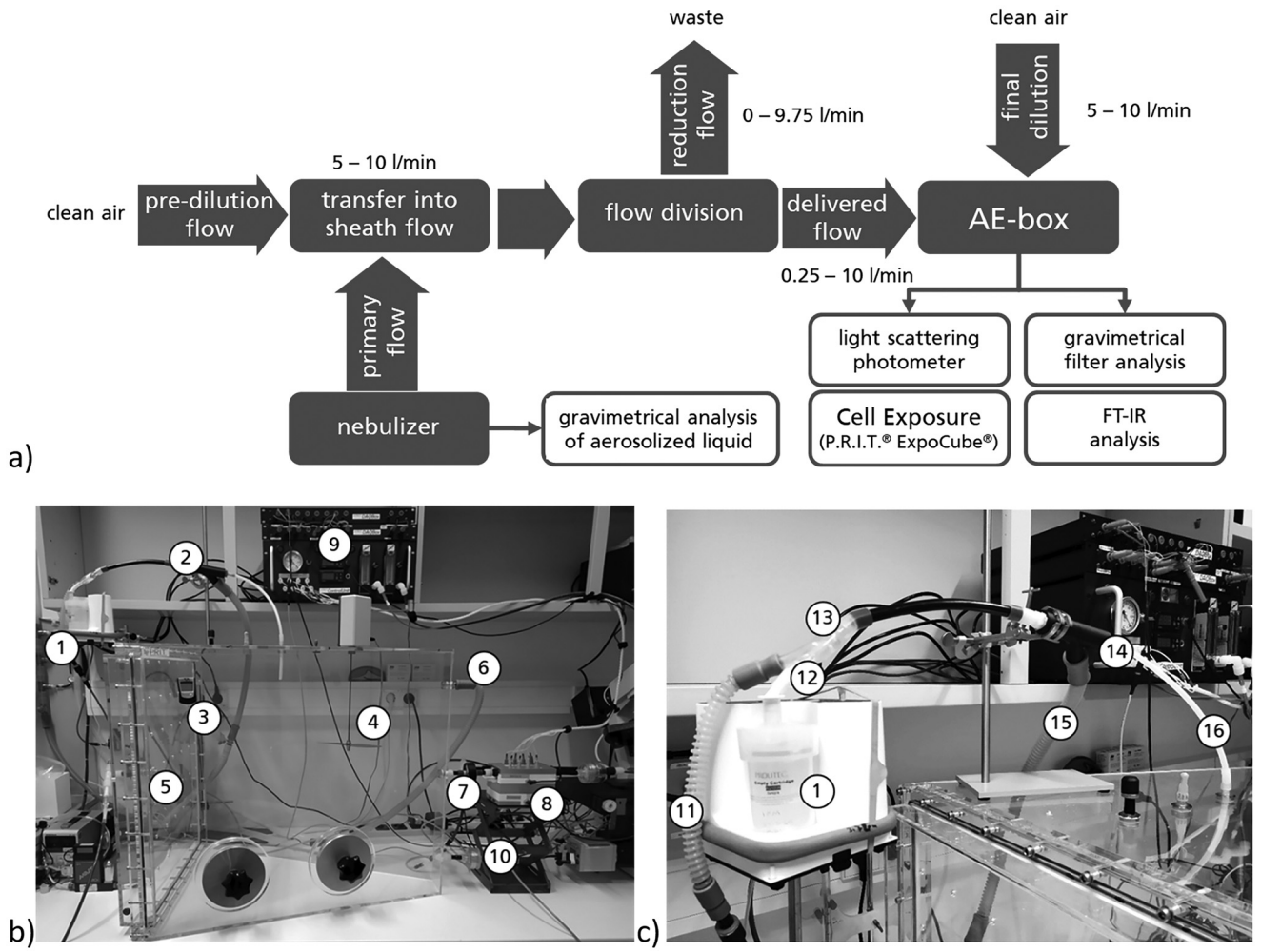


**Figure 2.** Concept (a) and realization of aerosol generation and cell exposure (b,c). (1) Nebulizer and cartridge, (2) dilution system, (3) temperature and humidity control inside AE-Box, (4) ventilator, (5) final dilution flow, (6) box waste flow, (7) custom light scattering photometer, (8) P.R.I.T® ExpoCube®, (9) exposure control (flows, temperature), (10) filter and FT-IR sampling (11) sheath air flow, (12) primary aerosol delivery, (13) pre-dilution, (14) division of aerosol flow, (15) generation waste flow, (16) delivered flow into AE-Box.

phase concentration'), a FT-IR method was set up allowing for analysis of relative changes in gas concentrations. A mobile FT-IR analyzer (Gasmet DX4000) was used to determine the FT-IR spectrum of the complex gas mixture generated by nebulizing the fillings. Following basic principles of FT-IR gas analysis methods from complex mixtures such as DIN 38409-18:1981-02 (1981), the IR-extinction at 2933 $cm^{-1}$ was analyzed, representing unspecific C-$H_x$ vibrations.

### *Cell culture*

The human A549 cell line (ATCC®CCL-185™) was purchased from American Type Culture Collection (ATCC; LGC Promochem). Cells were routinely taken from a stock pool and grown in 75 $cm^2$ flasks by use of Dulbecco's MEM medium (Seromed, Berlin) supplemented with 10% fetal bovine serum (FBS) and antibiotics (0.01% Gentamicin) at 37 °C in a humidified atmosphere containing 5% $CO_2$. Cells were passaged every 3–4 days. During each passage, microscopic observation was conducted and cell quality and quantity were checked by use of an electronic cell counter (CASY® Cell Counter + Analyzer System; Schärfe System, Reutlingen, Germany). During a cell passage an aliquot of the cells was seeded on microporous membranes (0.4 µm 1 $cm^2$; BD Falcon). Cells were cultivated on membranes for approximately 72 h until they reached a confluent monolayer as inspected by light microscopy. Serum was removed from the culture during a medium change 18 h before exposure and residual liquid from the apical side of the cell layer. After exposure, A549 ALI-cultures were incubated under cell-specific conditions in a cell culture incubator for 24 h.

### *Cell exposure*

Cells were exposed using an exposure device for air-liquid interface exposure under optimized conditions (P.R.I.T.® ExpoCube®, Ritter and Knebel 2014). Briefly, ten A549 ALI cultures were transferred into the device in a 12-well plate and subject to aerosol exposure organized in three different experimental groups per plate. Four wells were exposed to the test aerosol, two wells served as non-exposure controls without exposure flow and four wells were exposed to clean

air. Clean air and test aerosol exposures took place using an exposure flow of 3 ml/min during application of a thermal gradient of 15 °C (cell temperature 35 °C, aerosol temperature 50 °C). The thermal gradient produces thermophoresis conditions, enabling effective deposition of small particles on the cellular surfaces and homogeneous deposition rates for particles especially in the size range below 1000 nm independent of their individual aerodynamic size (Ritter et al. 2018). Cell exposures were conducted for 60 min. Values for a number of exposure and dose related parameters were determined, including total mass concentration (nebulized material in gas and aerosol phase [mg/m$^3$]), actual aerosol concentration [mg/m$^3$] or surface dose (delivered aerosol mass on the cellular surface [µg/cm$^2$]). Surface dose was calculated from actual aerosol concentration using the exposure device specific deposition rate of 80% for particle-sizes larger than 2 µm (Ritter et al. 2018 and unpublished data) according to Equation 1.

$$SD = \frac{DR}{100} \times c_{aer} \times Q_{expo} \times t_{expo}$$

Equation 1: Calculation of surface dose in cell exposure experiments from aerosol concentration. $SD$ [µg/cm$^2$] = surface dose, $DR$ [%] = exposure-device specific deposition rate, $c_{aer}$ [µg/ml] = aerosol concentration $Q_{expo}$ [ml/(min × cm$^2$)] = exposure flow, $t_{expo}$ [min] = exposure time

### Cellular read-outs

Viability measurement, fluorescence imaging for MMP and unspecific stress and interleukin-8 analysis were conducted in a combined method from the same cultures.

#### Viability

Tetrazolium salt cleavage was analyzed at the end of a 24-h post-exposure incubation phase using a 10% WST-1 solution (Roche) in culture media. After 60 min reaction with the dye under cell-specific conditions in the incubator, 100 µl aliquots of the culture media were transferred into 96-well plates and absorption was determined in a multiwell reader (Spectramax plus 386, Molecular Devices, Sunnyvale, USA) at 450 nm with a reference wavelength of 690 nm.

#### Live-fluorescence imaging

Before cell exposure, cultures were stained with JC-1 (Molecular Probes) and Hoechst 33258 (Sigma Aldrich) live-fluorescence stains. Therefore, ALI cultures were incubated for 60 min apically with 250 µl Medium C including 5 µg/ml JC-1 and 10 µg/ml Hoechst 33258. Dye solution was removed and cells were washed once with warm PBS. At times of analysis immediately after exposure (0 h) and following to a 24-h post-exposure incubation phase (24 h), cultures were transferred to a high content screening system (Olympus ScanR) and fluorescence scanning was conducted at a 10× magnification (Olympus UPlanSApo 10×/0.40) using 3 fluorescence channels (Hoechst 350/450 nm, JC-1 non-polarized 480/520 nm, JC-1 polarized 565/595 nm). Images were analyzed using an Olympus ScanR-software package (ScanR Analysis version 3.01) in a custom image analysis process by defining regions of interest (ROIs) based on image edge-detection and channel-specific fluorescence intensities on the area of the cells. Intensities from the Hoechst channel contributed to the read-out 'unspecific stress.' A ratio of the fluorescence intensities was calculated from the JC-1 polarized to non-polarized measurements resulting in the mitochondrial membrane potential (MMP) read-out.

#### Interleukin 8

Interleukin 8 was measured using an ELISA-based commercial kit (R + D Systems). 100 µl aliquots of culture media were sampled at 24 h after exposure and analyzed according to the protocol of the manufacturer using a microplate absorption reader (Spectramax plus 386, Molecular Devices, Sunnyvale, USA) and a calibration curve between 125 and 2000 pg/ml IL-8.

### Statistical calculations

Percentage of control values was calculated from viability, MMP, unspecific stress and interleukin-8 data raw data using Microsoft Excel (Microsoft Office Professional Plus 2013). Results from exposures to the test item were referenced to clean air exposures. Means were calculated from read-outs of four technical replicates exposed in parallel and represented the result of one independent experiment. Mean values and standard deviations for repetitions of independent experiments were calculated for each standard exposure scenario. Best-fit regression analysis including the calculation of confidence levels at 95% was carried out using statistical software (OriginPro 2021b, OriginLab Corporation, Nothampton, USA) for dose-response data from nebulized filling #1. Applied models for fitting are given in the result figures. Results from alternative scenarios were considered significantly different when outside the 95% confidence interval of the dose-response fit from the filling #1 exposures. LOAELs were defined by the first dosimetric values from the 95% confidence interval of a best-fit that were correlated to <100% (MMP) or > 100% (stress, IL-8) of control effect.

## Results

### Aerosol characterization

The primary aerosol was generated by the nebulizer at 1.35 lpm aerosol flow and 6–15 mg/min depending on filling type and resulted in a mean particle size of 6.0 µm as determined by laser diffraction. Against that, particle size analysis from the nebulized TM1 at CL2 (160 mg/m$^3$) sampled from the AE-Box resulted in a mean MMAD of 3.12 µm and a geometrical standard deviation of 1.42 µm. Results from analysis of total mass concentrations, actual aerosol concentrations and relative gas-phase and aerosol concentrations in comparison of the concentration levels using TM1 are presented in Figure 3.

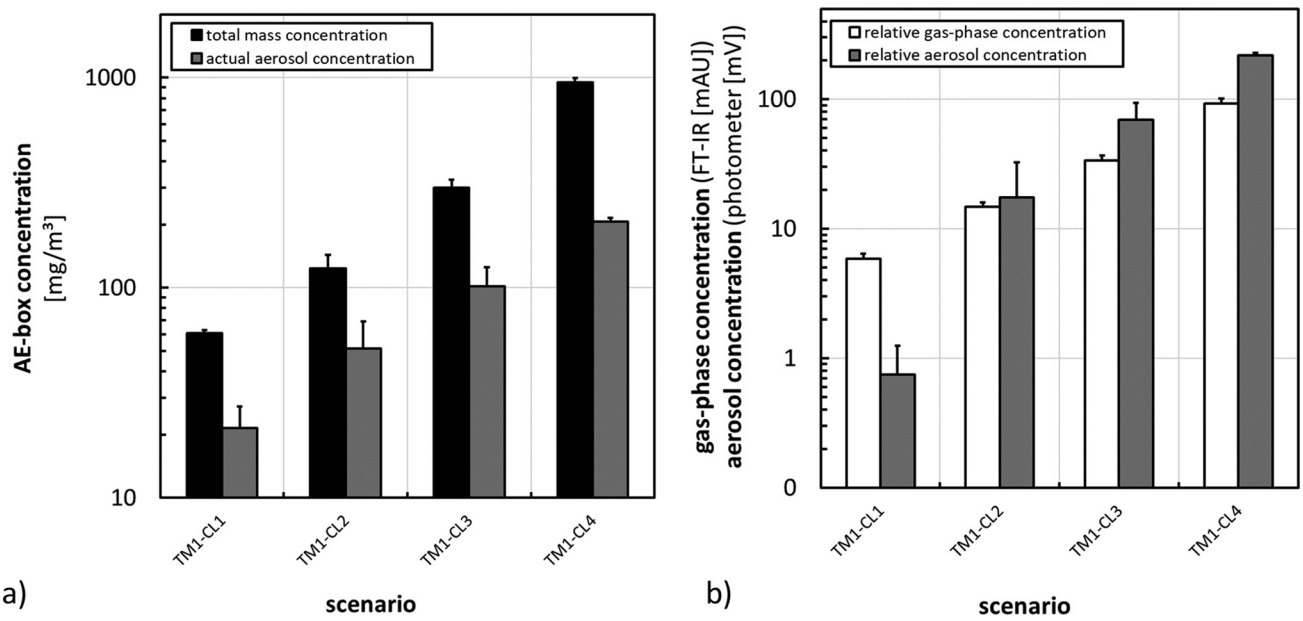


**Figure 3.** Results from aerosol characterization during application of basic scenarios using TM1 at different concentration levels. (a) Total mass and actual aerosol concentration inside the AE-box. (b) Relative results from gas-phase analysis by FT-IR and aerosol concentration measurement by light scattering carried out in front of the exposure device.

The results show that the targeted total mass concentrations according to Table 1 could be successfully realized in the AE-Box. Differences between the total mass concentration and actual aerosol concentrations are assumed to be a result of losses during aerosol transport and sampling from the AE-Box or partial evaporation of the nebulized substances into the gas-phase. Strong evaporation effects, however, are also indicated by the analyzed large reduction in mean aerosol particle size from 6 µm to 3.12 µm between the primary aerosol and the aerosol present in the AE-Box and therefore assumed to be the most prominent reason. Comparison of the aerosol recovery between total mass and actual aerosol concentrations for the different scenarios indicates a relatively stronger loss of aerosol material at the highest concentration (Figure 3(a), recovery between 33% and 41% for TM1 at CL1, CL2 and CL3, but 22% for CL4) and may be a result of higher losses due to transport, agglomeration and deposition at the highest concentration. Relative gas-phase concentrations in comparison to relative aerosol concentration, however (Figure 3(b)), were highest in CL1, whereas this ratio was changing only to a low extend with higher concentrations. A more effective evaporation at lower concentrations due to higher difference to a given saturation concentration-level in air, or a relatively higher loss of aerosol at the lowest concentration level on the transport from AE-box to cell exposure may be discussed as reasons for this observation. However, since the photometer signal was used a relative signal, quantitative interpretation should be carefully done.

Results from aerosol analysis during application of additional scenarios characterized the qualities of the different aerosols generated during filtering of nebulized TM1, from the pure main component from TM1 and from TM2 (Figure 4): (I) at comparable total mass-, actual aerosol- and gas-phase concentrations to the non-filtered scenario with TM1 (Figure 3) inside the AE-box, filtration was effective to reduce the aerosol concentration to non-detectability for cell exposure. (II) In comparison to nebulization of complete TM1, nebulization of the pure main component from TM1 only, resulted in comparable actual aerosol concentrations in the box and relative aerosol concentrations at the point of sampling for the cell exposure, but significantly reduced gas-phase concentrations at the same time. (III) Against that, nebulization of TM2 resulted in comparable total mass- and gas-phase concentrations to nebulization of TM1, but significantly reduced actual and relative aerosol concentrations.

## *Cellular read-outs*

### *Viability*

None of the test scenarios resulted in a significant reduction of cellular viability (WST-1) of exposed cells in comparison to clean air controls after 24 h except for exposures at the highest concentration-level using nebulized pure main component of TM1 (TM1-CL4), where a weak effect of 89.66 ± 3.34% of control was found.

### *Mitochondrial membrane potential (MMP)*

The effect of cell exposures toward nebulized TM1 at the four concentration-levels on the MMP immediately (0 h) or 24 h after exposure is shown in Figure 5. The results were plotted against the experimental total mass concentrations as dose-metric and evaluated statistically by calculation of a dose-response-fitting with 95% confidence intervals.

Except for exposures to the lowest aerosol concentration (60 mg/m$^3$), all other exposure scenarios resulted in concentration depending depletion of the MMP immediately after exposure to nebulized TM1 and even more pronounced following to the 24 h post-exposure incubation period.

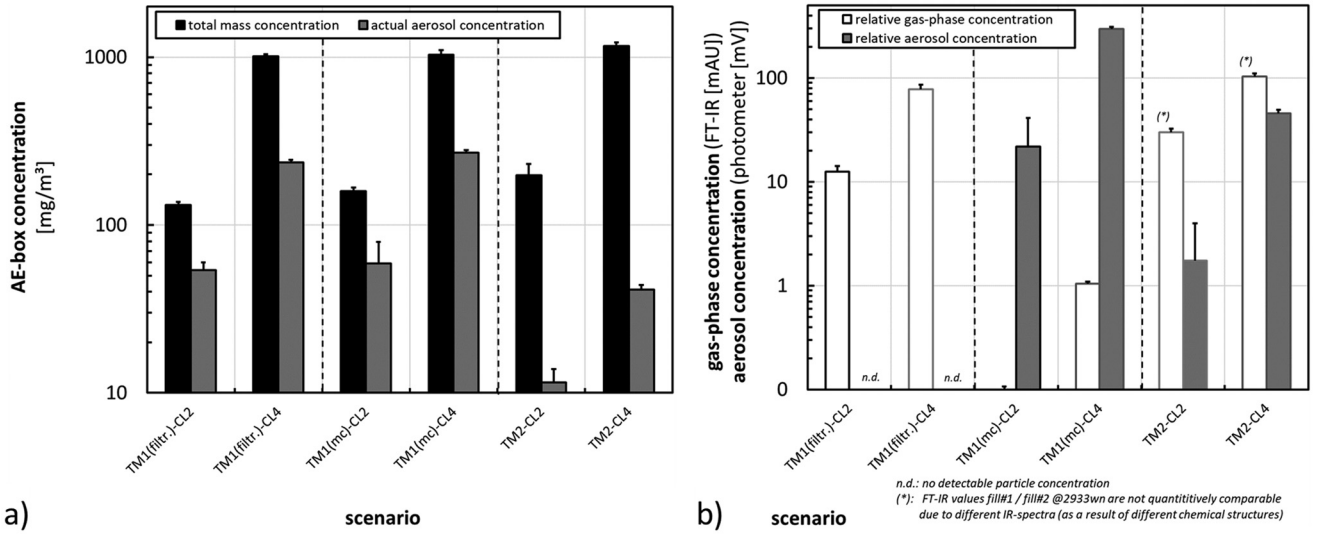


**Figure 4.** Results from aerosol characterization during application of additional scenarios. (a) Total mass and actual aerosol concentration inside the AE-box. (b) Relative gas-phase and aerosol concentrations during sampling for cell exposure after filtering of aerosols from TM1 (TM1(filtr)), with the pure main component from TM1 (TM1(mc)) or during nebulization of TM2 at different concentration levels (CL2 or CL4).

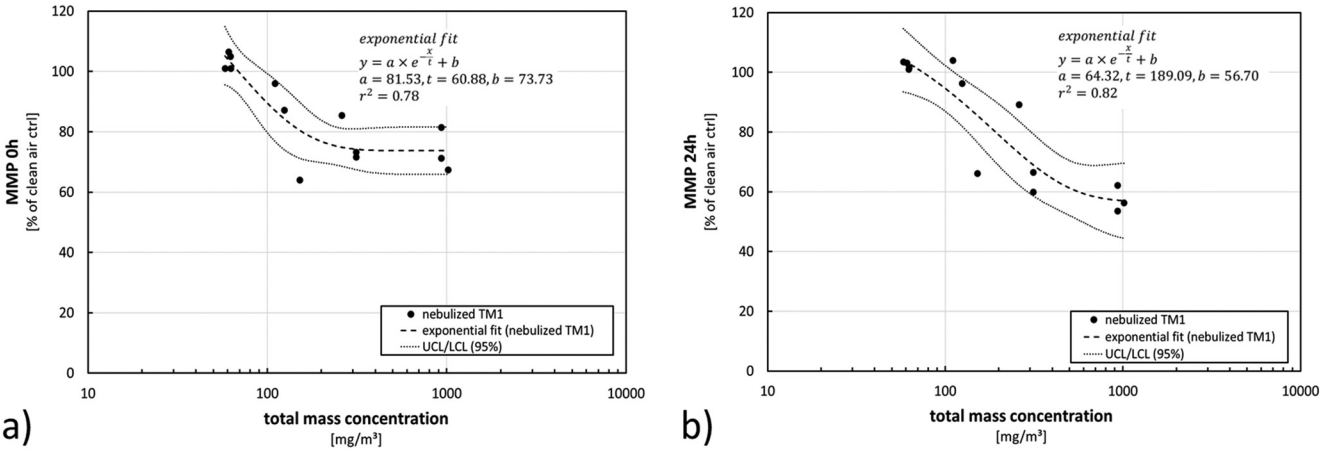


**Figure 5.** Effects on the cellular mitochondrial membrane potential (MMP) after exposure to nebulized TM1 at different concentration levels. (a) Measurement immediately after exposure (0 h); (b) measurement following to a 24-h post-exposure incubation phase. Results are presented as percentage of control in comparison to clean air controls. Dots represent results from single exposure experiments. Statistical best-fit analysis with 95% upper and lower confidence intervals (UCL, LCL).

These results from exposures toward nebulized TM1 are compared to results from testing nebulized TM1 after filtering (TM1(fitr.)), nebulized pure main component of TM1 (TM1(mc)) and nebulized TM2 (TM2) in Figure 6 by compilation of the dose-response fit from testing nebulized TM1 with confidence intervals according to Figure 5 and the results from single experiments of the other scenarios.

In agreement with the MMP data from both times of analysis, exposures to filtered aerosol from TM1 and exposures to nebulized TM2 resulted in significantly lower depletion of the MMP than exposures to complete aerosol from nebulization of TM1. MMP effects from exposures to the nebulized pure main component from TM1 were comparable to the effects from complete TM1 aerosol.

### *Unspecific stress*

Exposures to nebulized TM1 induced unspecific cellular stress at different levels, depending on aerosol concentration and timepoint of analysis (Figure 7).

Immediate cellular response is indicated by the cellular stress data and was detected for all but the lowest concentrations from nebulizing TM1. Higher concentrations induced a low and non-concentration dependent response immediately after exposure and strong concentration-depending inductions of cellular stress 24 h later.

Following the same concept of data evaluation as introduced for the MMP above, unspecific stress data from exposures to nebulized TM1 is presented in Figure 8 for comparison to the results from exposures to filtered aerosol from nebulized TM1, to nebulized pure main component from TM1 or nebulized TM2.

Effects on cellular stress were less pronounced immediately after exposure in comparison to 24 h later. Consequently, the measurement at 24 h characterized the discriminating effects on the cellular stress induced by the different exposure scenarios more clearly. Immediately after exposure, all but exposures to filtered aerosol from nebulized TM1 induced a small effect. 24 h later, exposures to filtered aerosol from nebulizing

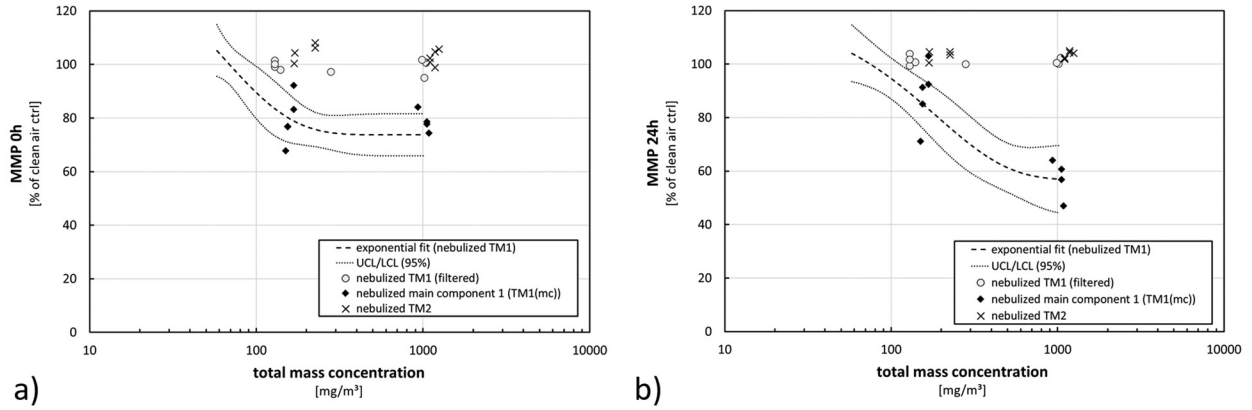


**Figure 6.** Results from analysis of the mitochondrial membrane potential (MMP) immediately after exposure (0 h) (a) or 24 h later (b). Fit (dashed line) with confidence interval at a level of 95% (dotted lines) represent the results from exposures toward nebulized TM1 (Figure 5). Results from single experiments using additional scenarios are shown in comparison (open circles = nebulized TM1 (filtered), black diamonds = nebulized main component from TM1, crosses = nebulized TM2). Total mass concentrations during filtered scenarios refer to the related AE-box concentrations during these exposure scenarios before filtering. Results not lying within the confidence interval from the TM1 fit are considered as significantly different.

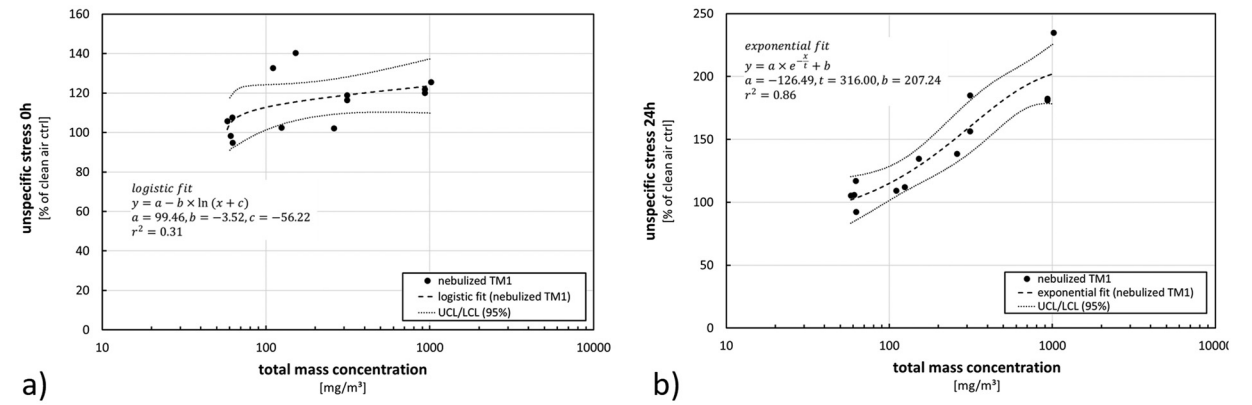


**Figure 7.** Effects on cellular stress after exposure to nebulized TM1 at different concentration levels. (a) Measurement immediately after exposure (0 h); (b) measurement following to a 24-h post-exposure incubation phase. Results are presented as percentage of control in comparison to clean air controls. Dots represent results from single exposure experiments. Statistical best-fit analysis with 95% upper and lower confidence intervals (UCL, LCL).

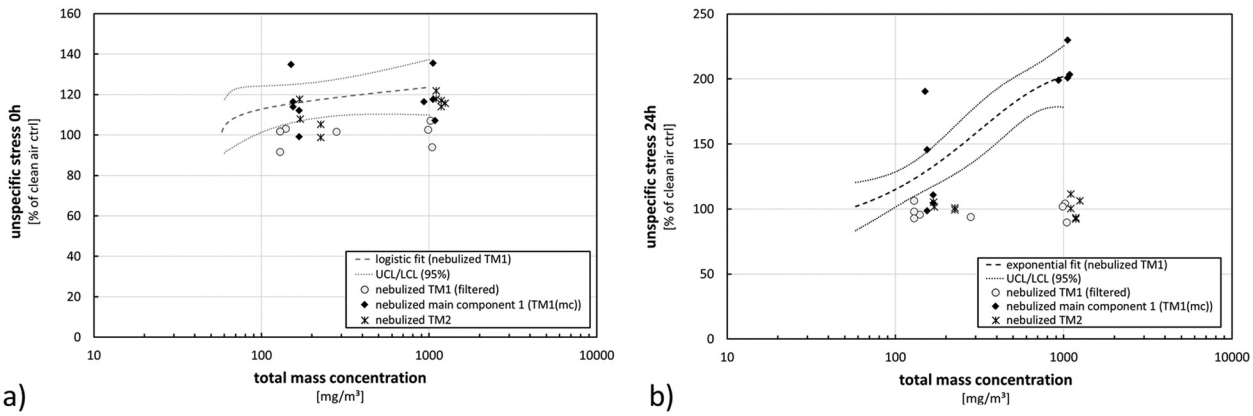


**Figure 8.** Results from analysis of cellular stress immediately after exposure (0 h) (a) or 24 h later (b). Fit (dashed line) with confidence interval at a level of 95% (dotted lines) represent the results from exposures toward nebulized TM1 (Figure 7). Results from single experiments using additional scenarios are shown in comparison (open circles = nebulized TM1 (filtered), black diamonds = nebulized main component from TM1, crosses = nebulized TM2). Total mass concentrations during filtered scenarios refer to the related AE-box concentrations during these exposure scenarios before filtering. Results not lying within the confidence interval from the TM1 fit are considered as significantly different.

TM1 as well as to aerosols from nebulization of TM2 resulted in a significantly reduced cellular effect in comparison to exposures to nebulized TM1. Again (as it was the case for MMP), exposures to nebulized pure main component from TM1 resulted in comparable results with exposures toward nebulized complete TM1.

### *Interleukin 8*

Interleukin 8 was measured 24 h after exposure and results for exposures to nebulized TM1 at different concentrations are presented in Figure 9. With the exception of results from the lowest concentration level at 60 mg/m$^3$ they indicate a strong, concentration-dependent increase of IL-8 release.

Comparison of this data with results from exposures using filtered aerosol from nebulized TM1, the nebulized pure main component of TM1 or TM2 resulted in comparable observations to those after analysis of effects on MMP and cellular stress (Figure 10). The strong dose-responsive effects from exposures to complete aerosol after nebulization of complete TM1 were significantly reduced after exposures to filtered aerosol from TM1 or nebulization of TM2. Comparable, in single experiments even slightly higher effects were found after exposures to the nebulized pure main component from TM1.

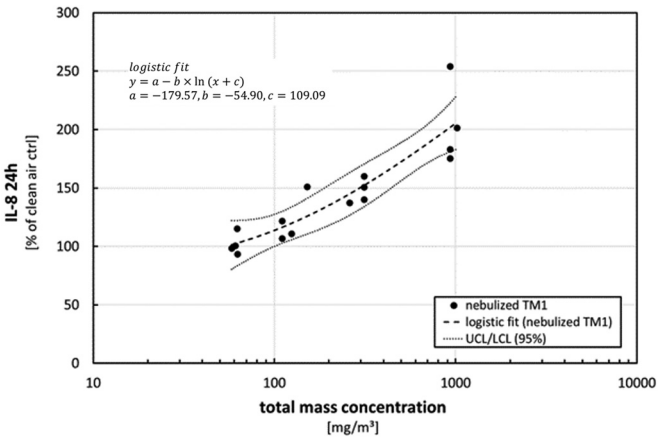


**Figure 9.** Effects on IL-8 release after exposure to nebulized TM1 at different concentration levels. Measurements following to a 24-h post-exposure incubation phase. Results are presented as percentage of control in comparison to clean air controls. Dots represent results from single exposure experiments. Statistical best-fit analysis with 95% upper and lower confidence intervals (UCL, LCL).

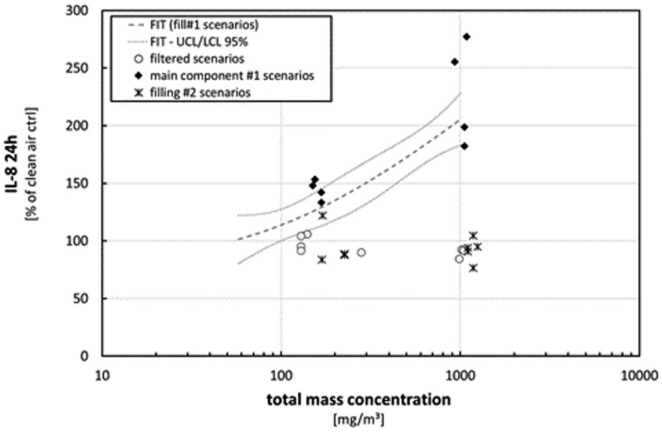


**Figure 10.** Results from analysis of Il-8 release within 24 h after exposure. Fit (dashed line) with confidence interval at a level of 95% (dotted lines) represent the results from exposures toward nebulized TM1 (Figure 9). Results from single experiments using additional scenarios are shown in comparison (open circles = nebulized TM1 (filtered), black diamonds = nebulized main component from TM1, crosses = nebulized TM2). Total mass concentrations during filtered scenarios refer to the related AE-box concentrations during these exposure scenarios before filtering. Results not lying within the confidence interval from the TM1 fit are considered as significantly different.

## Discussion

### *Basic concept*

Aerosols generated from different fillings of a commercial nebulizer were subject to evaluation of potential biological effects upon inhalation using an *in vitro* inhalation test system. Fillings represented potential products for commercial use in purposeful room conditioning and data on the nature and composition of the fillings were limited. TM1 was treated as a potential 'reference product' and *in vitro* inhalation effects from the nebulized TM1 were compared to *in vitro* inhalation effects from application of exposure scenarios including variation of product composition or aerosol treatment. Variations in aerosol treatment included setup of different aerosol concentration-levels referenced to real application and filtering of the aerosol generated by usage-relevant nebulization. Variations in product composition included testing of aerosols generated from the pure main component of TM1 only and from a second test material TM2, which was composed of an alternative main component 2, but the same active ingredient mix that was present in TM1 (Table 1).

Aerosol concentration levels during *in vitro* inhalation testing were referenced to real application based on the commercial nebulizer use as recommended by the manufacturer in a 'worst-case scenario.' This included the assumption that the material nebulized during a 24-h period of use would completely stay airborne, which is unlikely due to naturally occurring processes such as evaporation, agglomeration and gravitational deposition on walls, floor and furniture leading to an equilibrium concentration between aerosol generation and depletion and, consequently, to a much lower concentration. To achieve concentration-dependent testing of the aerosol, this basic worst-case concentration of 160 mg/m$^3$ was varied to higher and lower concentrations between 60 mg and 900 mg/m$^3$.

### *Aerosol characterization*

Observations from aerosol characterization attributed discriminating properties to aerosols from nebulization of TM1, of the pure main component from TM1, or TM2 or after filtering the aerosol from nebulization of TM1, especially regarding the presence of the 2 filling components (main component and the active ingredient mix) in the resulting gas- or aerosol phases after nebulization. Nebulization of the pure main component of TM1 resulted in comparable aerosol concentrations in comparison to the nebulization of complete TM1 but significantly lower gas-

**Table 2.** Assignment of components of the nebulized materials to the respective aerosol phases at the different exposure scenarios as a result of the aerosol characterization.

| Scenario | Composition | Assignment to nebulized aerosol phases | |
|---|---|---|---|
| TM1 | Main component 1 | Aerosol phase | ⇨ main component 1 |
| | Active ingredient mix | Vapor phase | ⇨ active ingredient mix |
| TM1 (mc) | Pure main component 1 | Aerosol phase | ⇨ main component 1 |
| | | Vapor phase | ⇨ *negligible* |
| TM1 (filtered) | Main component 1 | Aerosol phase | ⇨ *negligible* |
| | Active ingredient mix | Vapor phase | ⇨ active ingredient mix |
| TM2 | Main component 2 | Aerosol phase | ⇨ main component 2 |
| | Active ingredient mix | Vapor phase | ⇨ main component 2 + active ingredient mix |

phase concentrations at the same total mass concentration-levels. Hence, it can be concluded that the main component 1 was mainly present in the aerosol phase, whereas the active ingredient mix from TM1 evaporated into the gas-phase to a large extent. Nebulization of TM2 resulted in significantly lower actual aerosol concentrations in comparison to TM1 at the same total mass concentration. Since both mixtures contain the identical active ingredient mix but different main components, this leads to the conclusion that the pure main component 1 had a significantly lower vapor pressure than main component 2 from TM2 (which was not tested as a single component) leading to a higher evaporation rate of its main component 2 from the aerosol phase into the gas-phase.

These simple observations were of highest value for further interpretation of the biological response during the *in vitro* inhalation testing since they offered the unique possibility to correlate product composition, aerosol characteristics after nebulization (Table 2) and biological effects.

### *Cellular effects*

None of the tested exposure situations induced a significant effect on viability as measured by the tetrazolium-based assay WST-1, except for a small effect (10.34% loss of viability against air control) after nebulization of the pure main component 1 at the highest concentration level, which was a highly elevated worst-case scenario. Tetrazolium-based assays such as WST-1 or MTT are generally seen as representatives for cell number and/or cellular viability (Slater et al. 1963; Berridge et al. 2005; Stockert et al. 2018). Hence, these assays are broadly used for determination of cell toxicity (Guertler et al. 2011) and discussed to be highly indicative of *in vivo* acute toxicity (Lim et al. 2021). As a result, the present experimental *in vitro* outcome indicates a lack of acute respiratory toxicity potential of the aerosols from the test items under realistic and elevated exposure concentrations. Due to the characteristics of the test items as potential real products, this finding is not too surprising, since it can be expected that the single components for fillings and the main components will have been checked by the producer based on relevant toxicity data bases (e.g. www.echa.eu). However, since combinational toxicity effects from complex mixtures cannot be predicted due to a lack of knowledge, a non-target testing approach such as described here, might be helpful to confirm the actual lack of acute respiratory toxicity of the complex mixture.

Models for detecting potential biological sub-acute effects upon inhalation, however, are by far harder to set up and established approaches are rarely to find. Sub-acute effects might result in changes in the immune-system or have long-term consequences for health, where the term 'sub-acute' in the context of *in vitro* approaches is usually referring to a dose-level below observation of effects on cell-viability. Several experimental *in vitro* approaches are under discussion and have been conducted to describe long-term aka 'chronic' effects on respiratory tissues, such as re-organization of the basolateral cells by chronic smoking (Gindele et al. 2020). Also, complex methods such as the guard assay (Malmborg and Borrebaeck 2017; Grundström and Borrebaeck 2019) have been established to identify skin or respiratory sensitizers by *in vitro* methods. However, all those experimental approaches involve relatively cost- and time-intensive biological models such as primary 3D-models or read-outs such as gene-expressions analysis and are hard to integrate into a more routine, cost- and time-effective study design. For the realization of routine-design and detection of sub-toxic effects as potential indicatives of long-term biological changes at the same time, two live-fluorescence endpoints which are commonly used in high content screening (HCS) methods and FACS analysis (Salvioli et al. 1997; Zuliani et al. 2003; Guan et al. 2004) were integrated together with analysis of IL-8 release. Especially IL-8 release from A549-cells showed promising predictivity for *in vivo* effects (Dwivedi 2018). The non-invasive MMP (Cossarizza et al. 1993) and stress live-fluorescence measurements were carried out in a repeated manner kinetically at two time-points from the same cultures and by that supported the routine-design. MMP is involved in several toxicological pathways such as apoptosis (Bedner et al. 1999; Kamal et al. 2015) and others. Also, evidence has been shown for the relevance of mitochondrial dysfunction for toxicity of various types of chemicals (Dreier et al. 2019). Hence, this read-out seems well-suited for indication for unspecific detection of potential biological effects. A similar situation has been found for the unspecific nucleus stress indicator. Analysis is based on DNA-stain intercalation where the intensity of the staining is generally depending on the accessibility of the nuclear DNA for the stain (Stokke and Steen 1986; Ligasová and Koberna 2021). During toxicological events, the DNA can be in a less dense packed, condensed or fragmented status in the nucleus (Majtnerova et al. 2021) due to activation of gene

transcription- repair and other mechanisms and, hence, accessibility and following fluorescence intensity is increased.

The results from determination of these three endpoints resulted in a conclusive picture with respect to biological effects correlated to exposure scenarios and concentration levels. Generally, and without exception, the lowest concentration-level did not lead to any detectable biological response according to a no observed effects level (NOEL). Exposures at higher concentrations induced immediate MMP reduction, immediate stress increase and enhanced interleukin-8 release in a concentration-dependent way after nebulization of the complete TM1 or the pure main component 1. Effects after exposure toward filtered nebulized TM1 or nebulized TM2 were significantly lower, indicating that gas-phase effects in this case were mainly not responsible for the detected sub-toxic exposure effects. It is noteworthy that effects from exposures toward nebulized TM1 and exposures toward the nebulized pure main component 1 fitted nearly quantitatively.

A comparable low increase of cellular stress was observed immediately after exposure to nebulized TM2 as it was observed after exposure to nebulized complete TM1. For TM1 exposures however, the effect persisted after 24 h in an enhanced and concentration-level dependent manner whereas it was only transient after exposure to nebulized TM2, thus, not being detectable at 24 h. This may be interpreted as observation of an immediate cellular response and complete cellular recovery only with TM2. Against that, exposures to filtered nebulized TM1 did not result in any observable biological changes.

Quantitatively, total mass concentrations during testing of pure main component 1 included 20% more of this material than during testing of nebulized TM1, since the latter was composed of 80% main component and 20% active ingredient mix. This small difference might be responsible for the slightly higher effects in the IL-8 release after exposure to nebulized pure main component 1 in comparison to results from nebulized TM1 on the basis of the total aerosol mass concentration (Figure 10), thus, emphasizing the basic conclusiveness of results.

In summary, following qualitative characteristics of the test materials can be described at this level of interpretation by combining results from aerosol characterization and *in vitro* inhalation dose-response:

I. No effects from nebulized TM1 indicating strong acute toxicity could be found
II. Nebulized TM1 induced sub-acute, concentration-level depending effects
III. A NOEL was found for the concentrations at 60 mg/m$^3$
IV. Effects from nebulized TM1 could mainly be attributed to the aerosol-phase, which, again, was mainly formed by the main component from TM1
V. Change of main component 1 to main component 2 clearly decreased biological response and aerosol concentrations at the same time.

As a consequence, an alternative main component was identified indicating a less harmful product during TM2 application under realistic use conditions.

### *Quantitative in vitro to in vivo extrapolation of results*

Whereas the foregoing discussion focused qualitative *in vitro* to *in vivo* prediction by conclusively attributing biological effects to single components from the complex set of test items, quantitative meaning of results has further to be discussed with the focus on two topics. (1) Discriminating biological effects between TM1 and TM2 could be based on different toxicological characteristics between main component 1 and main component 2 or a consequence of different dosimetric situations. (2) The relevance of the exposure situations tested here for the human real-life exposure (QIVIVE).

#### *Different response toward filling #1 and filling #2*

Significantly lower aerosol concentrations at the same level of total mass concentrations were produced during nebulization of TM2 in comparison to nebulization of TM1 or the pure main component 1 (Figure 4(a)). Moreover, any detected biological effect could be attributed to the aerosol phase of these testing scenarios. Conclusively, it seems reasonable to change the dose-metric in the biological dose responses (Figures 6, 8, and 10) from 'total mass concentration' to 'actual aerosol concentration.' This is shown in Figure 11 for the stress (24 h) and interleukin-8 release as the most pronounced detected biological effects.

Again, results from testing of nebulized TM1 are represented as fittings from statistical evaluation of results with 95% confidence limits. The resulting LOAELs were 60 and 40 mg/m$^3$ for stress and IL-8, respectively. Aerosol-concentrations above these LOAELs were not reached after nebulization of TM2 due to less aerosol formation at the same level of total mass concentration in comparison to TM1. It has been discussed above that this may be a result of a higher vapor-pressure of the main component 2 in comparison to the main component 1. As a conclusion, it cannot be decided from these data whether the reduced biological effects from nebulized TM2 are a result of different toxicological properties of the different main component or a result of different physico-chemical properties such as a lower vapor pressure leading to lower aerosol concentrations at the same level of total mass concentration.

#### *Quantitative in vitro to in vivo extrapolation of results*

To reach quantitative *in vitro* to *in vivo* extrapolation of the present *in vitro* results, two exposure-related topics are discussed. (a) More realistic estimation of real-life air concentrations during use of the nebulizer system and (2) *in vivo* dose estimation.

More realistic estimation of relevant room concentrations during real use can be achieved by considering naturally occurring aerosol phenomena like gravitational settling and deposition on walls, furniture, and floor as well as coagulation processes, at least as a part of a rough model. Such

mechanisms lead to decrease of the airborne aerosol concentration and *in summa* to a steady-state concentration between continuous aerosol generation and loss. This potential equilibrium concentration is dependent on several additional factors such as the room air exchange rate or the dispersion coefficient. The physical distance of the nebulizer to the human being as the receptor is also an important factor in this context. By taking these factors into account and applying basic principles of aerosol technology (Baron and Willeke 2001) equilibrium concentrations as displayed in Table 3 have been calculated.

Without including additional, individual room characteristics such as furniture, non-consistent air exchange flows or others, the results demonstrate significantly lower equilibrium aerosol concentrations than the originally assumed worst-case concentration of 160 mg/m$^3$ (total mass concentration) and 59.39 mg/m$^3$ (actual aerosol concentration) for nebulized TM1.

Since results attributed any biological effects to the aerosol-phase of the nebulized fillings only, gas-phase exposure will not be included into dosimetric evaluations for QIVIVE. Transfer of data from dose-response with 'total mass concentration' to 'actual aerosol concentration' as relevant dose-metric delivered LOAELs for the most sensitive biological read-outs stress (24 h) and IL-8 release. The relevant *in vitro* dose, however, is not represented by aerosol concentration but by aerosol deposition on the surface of the cells. Meanwhile, it is common sense that the surface dose can be a relevant dose-metric to translate *in vitro* to *in vivo* results quantitatively (Schmid and Cassee 2017). The *in vitro* surface dose (SD) at the LOAEL exposure situation can be calculated according to equation 1 using the exposure flow rate (3 ml/min), exposure time (60 min) and the specific deposition rate under the experimental conditions. The deposition rate using the P.R.I.T.® ExpoCube® exposure device is a conservative value which is mainly dependent on particle size and can be assumed 80% for the present 3.2 µm particles (Ritter et al. 2018). 8.64 µg/cm$^2$ or 5.76 µg/cm$^2$ aerosol surface doses resulted for *in vitro* LOAEL exposures for stress (24 h) and IL-8 read-outs, respectively.

As the corresponding *in vivo* values for QIVIVE, the inner lung surface load could be estimated for human exposure based on the equilibrium concentrations as presented in Table 3, the particle diameter of 3.2 µm and assuming an 8 h working day single exposure, a tidal volume of 0.8 l, a breathing rate of 16.5 l/min, and an inner lung

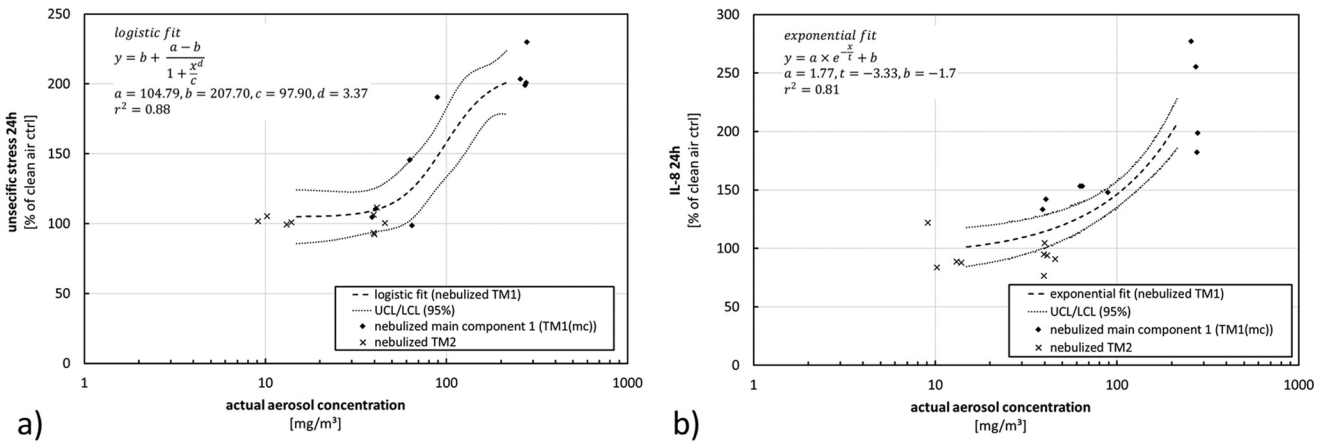


**Figure 11.** Results as presented in Figure 8(b) for stress and Figure 10 for interleukin-8 release transferred to the actual aerosol concentration as dose-metric.

**Table 3.** Estimation of more realistic room concentrations during nebulization using the given nebulizer at maximum output according to the manufacturers' manual in a 54 m$^2$ room for different use cases including variations of room air exchange rate and nebulizer to receptor distance.

| Case | Characteristic | Equilibrium aerosol concentration |
|---|---|---|
| Conservative | • Small distance nebulizer to receptor: 1 m<br>• Small dispersion coefficient: 0.01 m$^2$/s<br>• Air exchange rate 1/h | 3.69 mg/m$^3$ |
| Case 1 | Increased turbulent diffusion coefficient: 0.05 m$^2$/s | 2.25 mg/m$^3$ |
| Case 2 | Increased distance nebulizer to receptor:3 m | 1.92 mg/m$^3$ |
| Case 3 ('best case') | Increased air exchange rate: 5/h | 0.67 mg/m$^3$ |

**Table 4.** QIVIVE based on *in vivo* human exposure estimation and experimental *in vitro* inhalation LOAEL values.

| | *In vivo* | | | *In vitro* | | *In vitro/in vivo* |
|---|---|---|---|---|---|---|
| Estimation | Scenario | Equilibrium aerosol concentration | Surface dose | LOAEL | Surface dose | Factor |
| 'Pessimistic' | Conservative case | 3.69 mg/m$^3$ | 22.52 ng/cm$^2$ | 40 mg/m$^3$(IL-8) | 5.76 µg/cm$^2$ | 256 |
| 'Optimistic' | Case 3('best case') | 0.67 mg/m$^3$ | 4.1 ng/cm$^2$ | 60 mg/m$^3$(stress 24 h) | 8.64 µg/cm$^2$ | 2110 |

surface of 75 $m^2$ which are typical data for an average human being. A relative particle retention of 81.5%. was evaluated by application of MPPD software (Asgharian et al. 2001). 22.52 ng/$cm^2$ and 4.1 ng/$cm^2$ resulted from these calculations for the 'conservative' or 'case 3' use-cases representing the highest and lowest potential exposure levels in the exposure model.

*In vitro* dosages from the LOAEL exposure situations and *in vivo* dosages from the two use-cases are compared in Table 4. The calculated *in vitro*/*in vivo* factor represents the relative difference between the human lung exposure estimated for the use-cases on an 8-h working day and the onset of a biological effect as derived from the *in vitro* inhalation approach.

In the 'pessimistic' case, it would need a 256 times higher dosage to induce a biological effect in real-life exposure than from actual exposure estimated. However, for uncertainties during translational approaches such as translation from animal to human exposure, a safety factor of 100 would have to be applied during safety assessment, leaving a factor of 2.56 or 21.1 in the 'optimistic' case. Additionally, it must be considered that repeated exposures are likely such as exposure during following working days. Assuming a 5-day work week and a lack of knowledge on lung clearing mechanisms and ADME during that time, this situation might result in reaching the *in vitro*-derived LOAEL level.

Although having experimentally started with clearly unrealistic worst-case concentration-levels, the resulting data nevertheless delivered valuable information for a QIVIVE approach and showed that the potential onset of biological effects as determined *in vitro* might have relevance for the *in vivo* situation. Moreover, with TM2 an even less harmful potential design product could be identified based on the *in vitro* inhalation experimentation. This represents important data for safety assessment of product or product variations and may therefore be a valuable tool for safety assessment strategies in the future.

## Conclusion

The study shows how much information can be drawn on potential biological effects, *in vivo* relevance and the contribution of single components or individual aerosol compounds by application of a routine *in vitro* inhalation non-target testing approach although starting from a minimum of information on test materials and ending up in a QIVIVE approach. It is undoubtable that many uncertainties exist on the level of interpretation for conducting a QIVIVE approach such as experimental validation of the predictivity of the *in vitro* inhalation model, accuracy of LOAEL determination, human exposure estimation and others. However, it seems unrealistic that experimental validation by 'classic' approaches for such *in vitro* inhalation approaches could ever be carried out, since *in vivo* animal inhalation data are lacking even for single substances which in this case would also not help due to highly complex nebulized compounds and the need to translate to human exposure. Hence, it is expected that approaches like this will be of highest value for product safety and environmental health for inhalable products in the future, offering a high potential for toxicological interpretation at reasonable effort without any involvement of animal experimentation. Beyond that, growing knowledge from various applications might increase the certainty on *in vitro* to *in vivo* prediction and enhance further improvement of study design and interpretation of results.

## Acknowledgements

The authors thank Nico Sonnenschein for conducting interleukin-8 ELISA assays and laboratory work referring to cellular read-outs, Martin Engelke for carrying out the A549 cell culture, Martin Stempfle for doing parts of the aerosol characterization work, Andreas Hiemisch for carrying out cell exposure, FT-IR analysis and general aerosol characterization as well as high content screening application and lab organization. Furthermore, the authors thank Prof. Dr. Wolfgang Koch for facilitating calculations of equilibrium aerosol concentrations and valuable discussions on the respective aspects of the study.

## Disclosure statement

Rolf Fautz, Anne Zifle and Anne Fuchs are employees of a company selling cosmetic products, and providing the test items which are reported in the publication. All other authors are employees of the Fraunhofer Gesellschaft who is patentee of the ExpoCube® technology (DE 10 2013 109 450).

## Funding

The author(s) reported there is no funding associated with the work featured in this article.

## Data availability statement

The data that support the findings of this study are available from the corresponding author, Detlef Ritter, upon reasonable request.

## References

Asgharian B, Hofmann W, Bergmann R. 2001. Particle deposition in a multiple-path model of the human lung. Aerosol Sci Technol. 34(4): 332–339. doi: 10.1080/02786820151092478.

Baron PA, Willeke K. 2001. Aerosol measurement: principles, techniques, and applications. 2nd ed. Hoboken (NJ): John Wiley and Sons.

Bedner E, Li X, Gorczyca W, Melamed MR, Darzynkiewicz Z. 1999. Analysis of apoptosis by laser scanning cytometry. Cytometry. 35(3): 181–195. doi: 10.1002/(sici)1097-0320(19990301)35:3 < 181::aid-cyto1 > 3.0.co;2-5.

Berridge MV, Herst PM, Tan AS. 2005. Tetrazolium dyes as tools in cell biology: new insights into their cellular reduction. Biotchnol Annu Rev. 11:127–152. doi: 10.1016/S1387-2656(05)11004-7.

Bukowy-Bieryłło Z. 2021. Long-term differentiating primary human airway epithelial cell cultures: how far are we? Cell Commun Signal. 19:63. doi: 10.1186/s12964-021-00740-z.

Cossarizza A, Baccarani-Contri M, Kalashnikova G, Franceschi C. 1993. A new method for the cytofluorometric analysis of mitochondrial membrane potential using the J-aggregate forming lipophilic cation 5,5′,6,6′-tetrachloro-1,1′,3,3′-tetraethylbenzimidazolcarbocyanine Iodide (JC-1). Biochem Biophys Res Commun. 197(1):40–45. doi: 10.1006/bbrc.1993.2438.

DIN 38409-18:1981-02. 1981. German standard methods for the analysis of water. Waste water and sludge; Summary action and

material characteristic parameters (Group H); Determination of hydrocarbons (H 18).

Di Ianni E, Erdem JS, Møller P, Mønster Sahlgren N, Poulsen SS, Knudsen KB, Zienolddiny S, Saber AT, Wallin H, Vogel U, et al. 2021. *In vitro-in vivo* correlations of pulmonary inflammogenicity and genotoxicity of MWCNT. Part Fibre Toxicol. 18(1):25. doi: 10.1186/s12989-021-00413-2.

Dreier DA, Denslow ND, Martyniuk CJ. 2019. Computational *in vitro* toxicology uncovers chemical structures impairing mitochondrial membrane potential. J Chem Inf Model. 59(2):702–712. doi: 10.1021/acs.jcim.8b00433.

Dwivedi AM, Upadhyay S, Johanson G, Ernstgård L, Palmberg L. 2018. Inflammatory effects of acrolein, crotonaldehyde and hexanal vapors on human primary bronchial epithelial cells cultured at air-liquid interface. Toxicol in Vitro. 46:219–228. doi: 10.1016/j.tiv.2017.09.016.

FDA. 2022. Generally Recognized as Safe (GRAS). [last assessed 2022 Apr 28]. https://www.fda.gov/food/food-ingredients-packaging/generally-recognized-safe-gras.

Gindele JA, Kiechle T, Benediktus K, Birk G, Brendel M, Heinemann F, Wohnhaas CT, LeBlanc M, Zhang H, Strulovici-Barel Y, et al. 2020. Intermittent exposure to whole cigarette smoke alters the differentiation of primary small airway epithelial cells in the air-liquid interface culture. Sci Rep. 10(1):6257. doi: 10.1038/s41598-020-63345-5.

Grundström G, Borrebaeck CA. 2019. Skin sensitization testing—what's next? Int J Mol Sci. 20(3):666. doi: 10.3390/ijms20030666.

Hartung T. 2018. Perspectives on *in vitro* to *in vivo* extrapolations. Appl In Vitro Toxicol. 4(4):305–316. doi: 10.1089/aivt.2016.0026.

Guan X, Peng J-R, Yuan L, Wang H, Wei Y-H, Leng X-S. 2004. A novel, rapid strategy to form dendritomas from human dendritic cells and hepatocellular carcinoma cell line HCCLM3 cells using mature dendritic cells derived from human peripheral blood CD14+ monocytes within 48 hours of *in vitro* culture. World J Gastroenterol. 10(24):3564–3568. doi: 10.3748/wjg.v10.i24.3564.

Guertler A, Kraemer A, Roessler U, Hornhardt S, Kulka U, Moertl S, Friedl AA, Illig T, Wichmann E, Gomolka M. 2011. The WST survival assay: an easy and reliable method to screen radiation-sensitive individuals. Radiat Prot Dosimetry. 143(2–4):487–490. doi: 10.1093/rpd/ncq515.

Hallagan JB, Hall RL, Drake J. 2020. The GRAS provision - the FEMA GRAS program and the safety and regulation of flavors in the United States. Food Chem Toxicol. 138:111236. doi: 10.1016/j.fct.2020.111236.

Kamal A, Nayak VL, Bagul C, Vishnuvardhan MVPS, Mallareddy A. 2015. Investigation of the mechanism and apoptotic pathway induced by 4b cinnamido linked podophyllotoxins against human lung cancer cells A549. Apoptosis. 20(11):1518–1529. doi: 10.1007/s10495-015-1173-6.

Lieber M, Smith B, Szakal A, Nelson-Rees W, Todaro G. 1976. A continuous tumor cell-line from a human lung carcinoma with properties of type-II alveolar epithelial cells. Int J Cancer. 17(1):62–70. doi: 10.1002/ijc.2910170110.

Ligasová A, Koberna K. 2021. DNA dyes—highly sensitive reporters of cell quantification: comparison with other cell quantification methods. Molecules. 26(18):5515. doi: 10.3390/molecules26185515.

Lim SK, Yoo J, Kim H, Lim YM, Kim W, Shim I, Kim HR, Kim P, Eom IC. 2021. Prediction of acute inhalation toxicity using cytotoxicity data from human lung epithelial cell lines. J Appl Toxicol. 41(7):1038–1049. doi: 10.1002/jat.4090. Epub 2020 Oct 21. PMID: 33085125.

Lou J, Wang W, Lu H, Wang L, Zhu L. 2021. Increased disinfection byproducts in the air resulting from intensified disinfection during the COVID-19 pandemic. J Hazard Mater. 418:126249. doi: 10.1016/j.jhazmat.2021.126249.

Majtnerova P, Capek J, Petira F, Handl J, Rousar T. 2021. Quantitative spectrofluorometric assay detecting nuclear condensation and fragmentation in intact cells. Sci Rep. 11(1):11921. doi: 10.1038/s41598-021-91380-3.

Malmborg A, Borrebaeck CAK. 2017. Testing human skin and respiratory sensitizers—what is good enough? Int J Mol Sci. 18(2):241. doi: 10.3390/ijms18020241.

Mennecier G, Torres LN, Cogliati B, Sanches DS, Mori CM, Latorre AO, Chaible LM, Mackowiak II, Nagamine MK, Da Silva TC, et al. 2014. Chronic exposure of lung alveolar epithelial type II cells to tobacco-specific carcinogen NNK results in malignant transformation: a new *in vitro* lung carcinogenesis model. Mol Carcinog. 53(5):392–402. doi: 10.1002/mc.21987.

Nardone LL, Andrews SB. 1979. Cell line A549 as a model of the type II pneumocyte. Biochim Biophys Acta. 573(2):276–295. doi: 10.1016/0005-2760(79)90061-4.

Person RJ, Tokar EJ, Xu Y, Orihuela R, Olive Ngalame NN, Waalkes MP. 2013. Chronic cadmium exposure *in vitro* induces cancer cell characteristics in human lung cells. Toxicol Appl Pharmacol. 273(2):281–288. doi: 10.1016/j.taap.2013.06.013.

Ritter D, Bitsch A, Elend M, Schuchardt S, Hansen T, Brodbeck C, Knebel J, Fuchs A, Gronewold C, Fautz R. 2018. Development and evaluation of an *in vitro* test system for toxicity screening of aerosols released from consumer products and first application to aerosols from a hair straightening process. Appl In Vitro Toxicol. 4(2):180–192. doi: 10.1089/aivt.2017.0036.

Ritter D, Knebel J. 2014. Investigations of the biological effects of airborne and inhalable substances by cell-based *in vitro* methods: fundamental improvements to the ALI concept. Advances in Toxicology Volume. 2014:1–11. Article ID doi: 10.1155/2014/185201.

Salvioli S, Ardizzoni A, Franceschi C, Cossarizza A. 1997. JC-1, but not DiOC6(3) or rhodamine 123, is a reliable fluorescent probe to assess delta psi changes in intact cells: implications for studies on mitochondrial functionality during apoptosis. FEBS Lett. 411(1):77–82. doi: 10.1016/s0014-5793(97)00669-8.

Schmid O, Cassee FR. 2017. On the pivotal role of dose for particle toxicology and risk assessment: exposure is a poor surrogate for delivered dose. Part Fibre Toxicol. 14(1):52. doi: 10.1186/s12989-017-0233-1.

Selo MA, Sake JA, Kim K-J, Ehrhardt C. 2021. *In vitro* and ex vivo models in inhalation biopharmaceutical research—advances, challenges and future perspectives. Adv Drug Deliv Rev. 177:113862. doi: 10.1016/j.addr.2021.113862.

Slater TF, Sawyer B, Straeuli U. 1963. Studies on succinate-tetrazolium reductase systems. III. Points of coupling of four different tetrazolium salts. Biochim Biophys Acta. 77:383–393. doi: 10.1016/0006-3002(63)90513-4.

Srivastava S, Zhao X, Manay A A, Chen Q. 2021. Effective ventilation and air disinfection system for reducing coronavirus disease 2019 (COVID-19) infection risk in office buildings. Sustain Cities Soc. 75:103408. doi: 10.1016/j.scs.2021.103408.

Stockert JC, Horobin RW, Colombo LL, Blázquez-Castro A. 2018. Tetrazolium salts and formazan products in cell biology: viability assessment, fluorescence imaging, and labeling perspectives. Acta Histochem. 120(3):159–167. doi: 10.1016/j.acthis.2018.02.005.

Stokke T, Steen HB. 1986. Binding of Hoechst 33258 to chromatin in situ. Cytometry. 7(3):227–234. doi: 10.1002/cyto.990070302.

Upadhyay S, Palmberg L. 2018. Air-liquid interface: relevant *in vitro* models for investigating air pollutant-induced pulmonary toxicity. Toxicol Sci. 164(1):21–30. doi: 10.1093/toxsci/kfy053.

Vlaskin MS. 2022. Review of air disinfection approaches and proposal for thermal inactivation of airborne viruses as a life-style and an instrument to fight pandemics. Appl Therm Eng. 202:117855. doi: 10.1016/j.applthermaleng.2021.117855.

Zuliani T, Duval R, Jayat C, Schnebert S, André P, Dumas M, Ratinaud M-H. 2003. Sensitive and reliable JC-1 and TOTO-3 double staining to assess mitochondrial transmembrane potential and plasma membrane integrity: interest for cell death investigations. Cytometry A. 54(2):100–108. doi: 10.1002/cyto.a.10059.